AGU PUBLICATIONS

Geophysical Research Letters

RESEARCH LETTER
10.1002/2013GL058924

Key Points:
- ASR reproduce 35% cyclones more over the Arctic
- The most intense cyclones are deeper and have stronger winds in ASR
- Maximum of cyclone counts in central Arctic exists both in summer and in winter

Correspondence to:
N. Tilinina,
tilinina@sail.msk.ru

Citation:
Tilinina, N., S. K. Gulev, and D. H. Bromwich (2014), New view of Arctic cyclone activity from the Arctic system reanalysis, *Geophys. Res. Lett.*, *41*, 1766–1772, doi:10.1002/2013GL058924.

Received 2 DEC 2013
Accepted 3 FEB 2014
Accepted article online 7 FEB 2014
Published online 5 MAR 2014

New view of Arctic cyclone activity from the Arctic system reanalysis

Natalia Tilinina[1,2], Sergey K. Gulev[1,2], and David H. Bromwich[3]

[1]P.P. Shirshov Institute of Oceanology, Russian Academy of Sciences, Moscow, Russia, [2]Natural Risks Assessment Laboratory, Moscow State University, Moscow, Russia, [3]Byrd Polar Research Center, Ohio State University, Columbus, Ohio, USA

Abstract Arctic cyclone activity is analyzed in 11 year (2000–2010), 3-hourly output from the Arctic System Reanalysis (ASR) interim version. Compared to the global modern era reanalyses (European Centre for Medium-Range Weather Forecasts Reanalysis (ERA)-Interim, Modern Era Retrospective Analysis for Research and Applications, and National Centers for Environmental Prediction-Climate Forecast System Reanalysis), ASR shows a considerably higher number of cyclones over the Arctic with the largest differences over the high-latitude continental areas (up to 40% in summer and 30% in winter). Over the Arctic Ocean during both seasons ASR captures well the cyclone maximum in the Eastern Arctic which has 30% less cyclones in summer and is hardly detectable in winter in ERA-Interim. High resolution of the ASR model coupled with more comprehensive data assimilation allows for more accurate (compared to the global reanalyses) description of the life cycle of the most intense Arctic cyclones, for which ASR shows lower central pressure (4 hPa on average), faster deepening, and stronger winds on average.

1. Introduction

Arctic cyclone activity is of great interest due to its potential association with the large magnitude of Arctic warming and particularly unprecedented Arctic sea ice decline over the last decade [*Zhang et al.*, 2004; *Stroeve et al.*, 2007; *Deser et al.*, 2010; *Screen et al.*, 2011]. Some studies report a direct influence of very intense cyclones on the sea ice cover at synoptic time scales [*Simmonds and Rudeva*, 2012; *Zhang et al.*, 2013; *Parkinson and Comiso*, 2013]. Cyclone dynamics largely reflects atmospheric circulation changes potentially resulting from the amplification of the Arctic warming and possibly influencing midlatitude climate extremes such as droughts, extreme rainfall and flooding, cold spells, and heat waves over Eurasia and North America [*Francis and Vavrus*, 2012], although the role of different factors is quite controversial [*Barnes*, 2013; *Screen and Simmonds*, 2013]. Arctic cyclones also play an important role in high-latitude atmospheric heat and moisture transports. Importantly, this role may increase in the future climate due to the changing environmental conditions [*Screen et al.*, 2013].

Arctic cyclone activity is characterized by considerably different cyclone life cycle characteristics compared to midlatitude transients. High-latitude cyclones are typically smaller in size, shorter living, and more frequently experience rapid deepening [*Serreze*, 1995; *Gulev et al.*, 2001; *Rudeva and Gulev*, 2007; *Zhang et al.*, 2004]. With increased spatial resolution, existing modern era global reanalyses quite accurately and consistently with each other quantify midlatitude cyclone activity [*Hodges et al.*, 2011; *Tilinina et al.*, 2013], although some differences among them do exist due to different resolution and model formulations. However, the limited amount of assimilated data in high latitudes and suboptimal physics parameterizations in numerical weather prediction models used in global reanalyses lead to the uncertainties in capturing important regional mechanisms driving cyclone activity in the Arctic, first of all those, associated with boundary layer processes. Recently, *Shkolnik and Efimov* [2013] demonstrated high skill of a regional climate model (without data assimilation) in representing Arctic cyclone activity. In this respect the recently developed Arctic System Reanalysis (ASR) [*Bromwich et al.*, 2010] based on higher spatial resolution and assimilating considerably larger amounts of data compared to the global products (roughly 3 times more than European Centre for Medium-Range Weather Forecasts Reanalysis (ERA)-Interim over Arctic land) opens a new avenue in documenting Arctic cyclone activity. Here we present high-latitude cyclone activity as revealed by this new product and compare cyclone track density and characteristics of the cyclone life cycle in ASR with those in the global reanalyses. This will help to quantify whether the advances in ASR numerics (model setting) and data assimilation input resulted in significantly different characteristics of Arctic cyclone activity.

Table 1. Mean Seasonal (JASO, JFMA) Numbers of Cyclones (Count Per Season) Which Were Identified North of 55°N and Over the Arctic Ocean Area in the Four Reanalyses During the Period 2000–2010 and Basic Characteristics of the Reanalysis Data Sets Used in This Study

Season		JFMA			JASO		
Depth (hPa)		< 980 hPa	980–1000	> 1000 hPa	< 980 hPa	980–1000	> 1000 hPa
ASR (30 km, nonspectral L71, 3-hourly)	Arctic Ocean	31	53	20	24	75	26
	55°N	169	340	150	123	417	225
ERA-Interim (0.75° × 0.75°, T255L60, 6-hourly)	Arctic Ocean	25	50	19	20	65	19
	55°N	139	270	100	100	318	122
MERRA (1/2° × 2/3°, nonspectral L72, 6-hourly)	Arctic Ocean	26	52	18	22	64	18
	55°N	149	272	92	110	320	114
NCEP-CFSR (0.5° × 0.5°, T382L64, 1-hourly)	Arctic Ocean	27	52	18	23	65	20
	55°N	147	283	101	105	329	120

2. Data and Methods

ASR was performed with the high-resolution version of the nonhydrostatic Polar Weather Research and Forecast model (Polar Weather Research and Forecasting (WRF) V3.3.1) [*Bromwich et al*., 2009; *Hines et al*., 2011; *Hines and Bromwich* 2008; *Wilson et al*., 2012] using ERA-Interim reanalysis [*Dee et al*., 2011] data as lateral boundary conditions. ASR was produced using the WRF-data assimilation and high-resolution land data assimilation systems that have been optimized for the Arctic and assimilated much more data compared to standard assimilation input, particularly surface weather observations, and more accurate lower boundary condition descriptions over land and ocean that are frequently updated. In this study we used 3-hourly sea level pressure (SLP) from the ASR interim version (30 km spatial resolution, 360 × 360 points) for the 11 year period from 2000 to 2010. For comparison of the characteristics of cyclone activity we employed several modern era reanalyses, namely, National Centers for Environmental Prediction-Climate Forecast System Reanalysis (NCEP-CFSR) [*Saha et al*., 2010], ERA-Interim [*Dee et al*., 2011], and MERRA [*Rienecker et al*., 2011] for the same time period (Table 1).

Cyclone tracking was performed with a numerical algorithm developed at P.P. Shirshov Institute of Oceanology, Russian Academy of Sciences [*Zolina and Gulev*, 2002; *Rudeva and Gulev*, 2007; *Tilinina et al*., 2013], based on sea level pressure and comprehensively evaluated under the Intercomparison of Mid-Latitude Storm Diagnostics (IMILAST) project [*Neu et al*., 2013]. This scheme, originally designed for the polar orthographic grid, fits the arrangement of ASR output, so the tracking was performed directly on the ASR native grid. In order to eliminate small-scale noise in the ASR SLP fields primarily associated with orographic features, we applied a 2-D spatial Lanczos filtering [*Duchon*, 1979] with wave number cutoff equivalent to 100 km. In other respects the scheme was identical to that used earlier in numerous applications [*Neu et al*., 2013; *Tilinina et al*., 2013]. Prior to analysis we eliminated from the tracking output all transients with lifetime less than 12 h. Then we considered different thresholds on lifetime and migration (up to 3 days and 1500 km) and their impact on the results (section 3). We also filtered out all cyclones reaching minimum central pressure over elevated orography (higher than 1500 m) and cyclones generated in the areas higher than 1000 m over Greenland. This preprocessing is typically applied in most tracking algorithms while the thresholds may differ [*Neu et al*., 2013]. Most numerical schemes experience high uncertainties with identification of short-lived cyclones and cyclones over the complex terrain where the errors in the adjustment of pressure to sea level are large in most NWP products.

Tracking of the limited area domain (ASR) implies also the so-called entry-exit uncertainties resulting in the presence of cyclones generated or decaying outside the domain. To avoid the impact of these cyclones on the results, we considered only cyclone tracks entering 55°N latitude circle. Given that ASR domain covers the Northern Hemisphere at least north of 50°N going to 30°N in the southmost domain locations, this guarantees in most cases consideration of only cyclones with a complete life cycle and fits well to our focus on Arctic cyclone activity. Recently, *Shkolnik and Efimov* [2013] working with data assimilation free model embedded an inner grid into the outer domain of the global model solution for resolving entry-exit problem for limited area tracking. In our case this approach is not applicable because of the very different data assimilation approaches in ERA-Interim and ASR. To achieve the consistency in comparisons, a similar procedure has been applied to the tracking output from global reanalyses. To map spatial patterns of cyclone

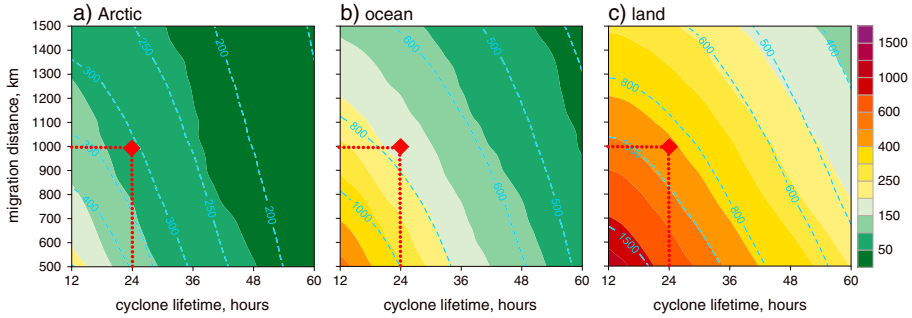

Figure 1. Annual differences in number of cyclones between ASR and ERA-Interim after applying different thresholds on cyclone lifetime and migration for (a) Arctic Ocean, (b) oceans, and (c) continents north from 55°N. Blue lines show the number of cyclones in ASR. Red diamonds mark the threshold used for all subsequent figures.

numbers, we applied a technique suggested by *Tilinina et al*. [2013], using a circular grid with circular cell area of 155,000 km^2 and a linear interpolation of tracks onto 10 min steps for minimization of the random and systematic biases in the results [*Zolina and Gulev*, 2002]. The results are presented for the two so-called "Arctic seasons" (January, February, March, and April (JFMA) and July, August, September, and October (JASO)), chosen for the periods of maximum and minimum Arctic sea ice cover, respectively.

3. Results

The annual number of cyclones identified by ASR is higher than in the modern era global reanalyses. However, the magnitude of differences depends on the thresholds used to eliminate short-lived transients. Relative difference between the total annual cyclone counts in ASR and ERA-Interim increases from 30 to 50% with the decrease of thresholds on lifetime and migration from 60 to 12 h and from 1500 to 500 km, respectively (Figure 1). This corresponds to the increase of absolute differences by a factor of 10 with the largest differences in the high-latitude continental areas and the smallest being for the so-called Arctic Ocean region (defined here as the ocean north of 65°N). Importantly, for all regions these differences are always

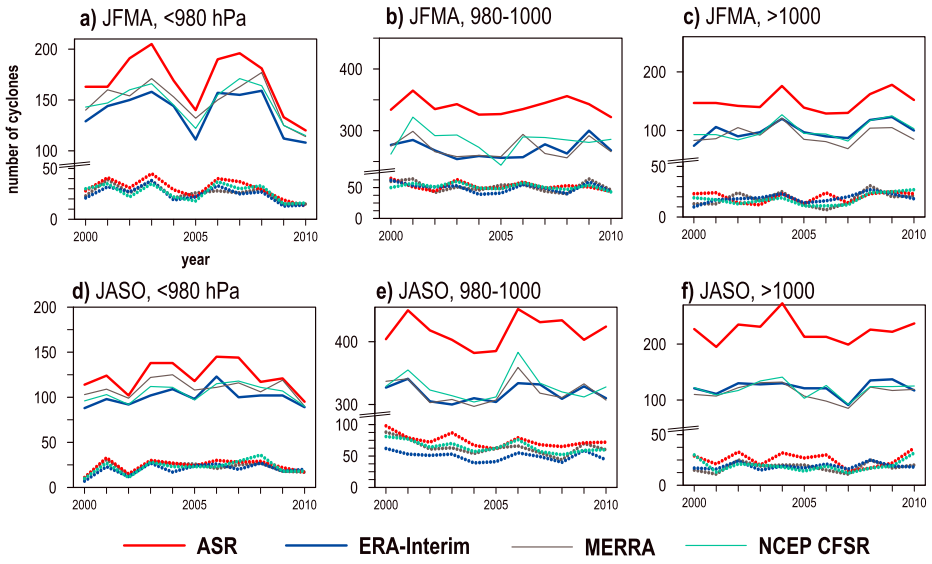

Figure 2. Time series of the annual number of (a and d) deep (central pressure smaller than 980 hPa), (b and e) moderate (central pressure is 980–1000 hPa), and (c and f) weak (central pressure is higher than 1000 hPa) cyclones for JFMA (Figures 2a, 2b, and 2c) and JASO (Figures 2d, 2e, and 2f) seasons in different reanalyses. Bold lines correspond to the number of cyclones within 55°N circle; dotted lines are for the cyclones over the Arctic Ocean area (see text for definition).

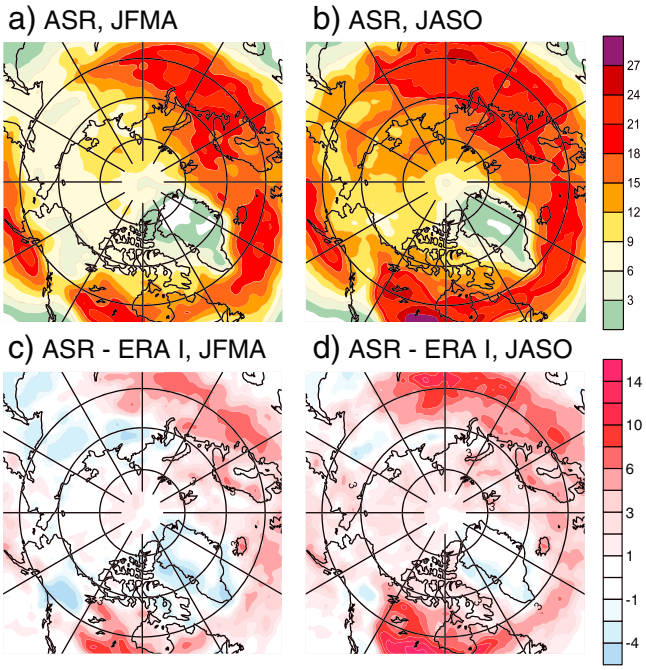

Figure 3. Seasonal climatologies (2000–2010) of cyclone numbers in (a and b) ASR and (c and d) differences in cyclone counts between ASR and ERA-Interim for (a and c) summer and (b and d) winter. Units are tracks per year per 155,000 km^2.

positive (ASR reports larger number of cyclones than ERA-Interim does) even for very strict thresholds. Here the results are presented for cutoffs at 24 h and 1000 km.

In both seasons ASR shows more cyclones than the three modern era reanalyses with the differences being about 28% in winter and almost 40% in summer (Figure 2 and Table 1). These differences are formed mostly by moderately deep and shallow cyclones (central pressure higher than 980 hPa), while the number of deep cyclones is more consistent among different data sets with ASR showing 17% higher counts in winter and summer. Differences between the total number of cyclones in ASR and in the three global reanalyses for both seasons are statistically significant at 99% level for the whole ASR domain, while across MERRA, CFSR, and ERA-Interim, the differences are statistically significant at the 90% level. For the Arctic Ocean region, the differences between ASR cyclone counts and the other reanalyses decrease to 9% being larger for deep cyclones in winter (24%) and for shallow cyclones in summer (35%). For this area overall differences in cyclone numbers between ASR and the other data sets are just slightly higher compared to those between the three global reanalyses (5–10%).

Thus, during the decade of 2000s, the major differences between ASR and the other reanalyses are formed due to the cyclones over continental Arctic and over the GIN (Greenland, Irminger, and Norwegian) Sea. This is clearly seen in seasonal climatologies of cyclone numbers (Figure 3) in ASR along with the differences between ASR and ERA-Interim cyclone counts. ASR reproduces the major storm tracks over the northern North Atlantic and the GIN Sea and also continental storm tracks identified in *Tilinina et al.* [2013] in five global reanalyses (Figures 3a and 3b). Regional differences between ASR and ERA-Interim cyclone counts (Figures 3c and 3d) are the largest over the continental storm tracks (30 and 45% in winter and summer, respectively) and amount to 30% in both winter and summer over the oceanic storm track aligning from the subpolar North Atlantic over the GIN Sea to the Barents and Kara Seas. Importantly, ASR clearly identifies a regional maximum (more evident in summer) of cyclone activity

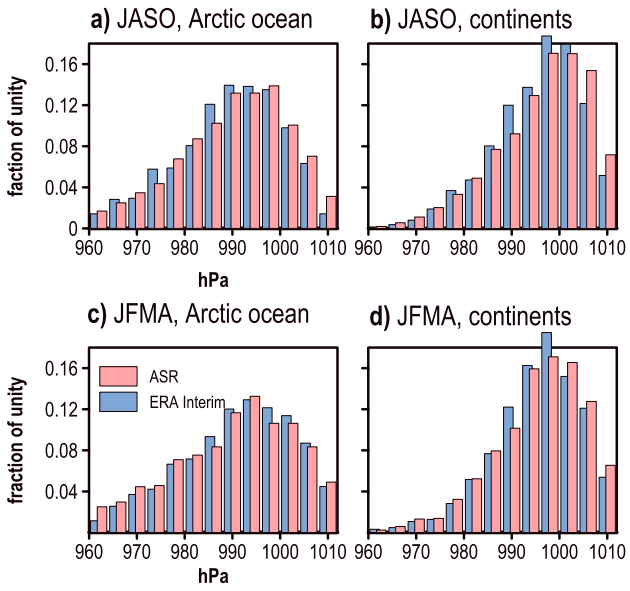

Figure 4. Climatological occurrence histograms of the minimum cyclone central pressure for the (a and c) Arctic Ocean area and (b and d) high-latitude continental areas for (a and b) summer and (c and d) winter.

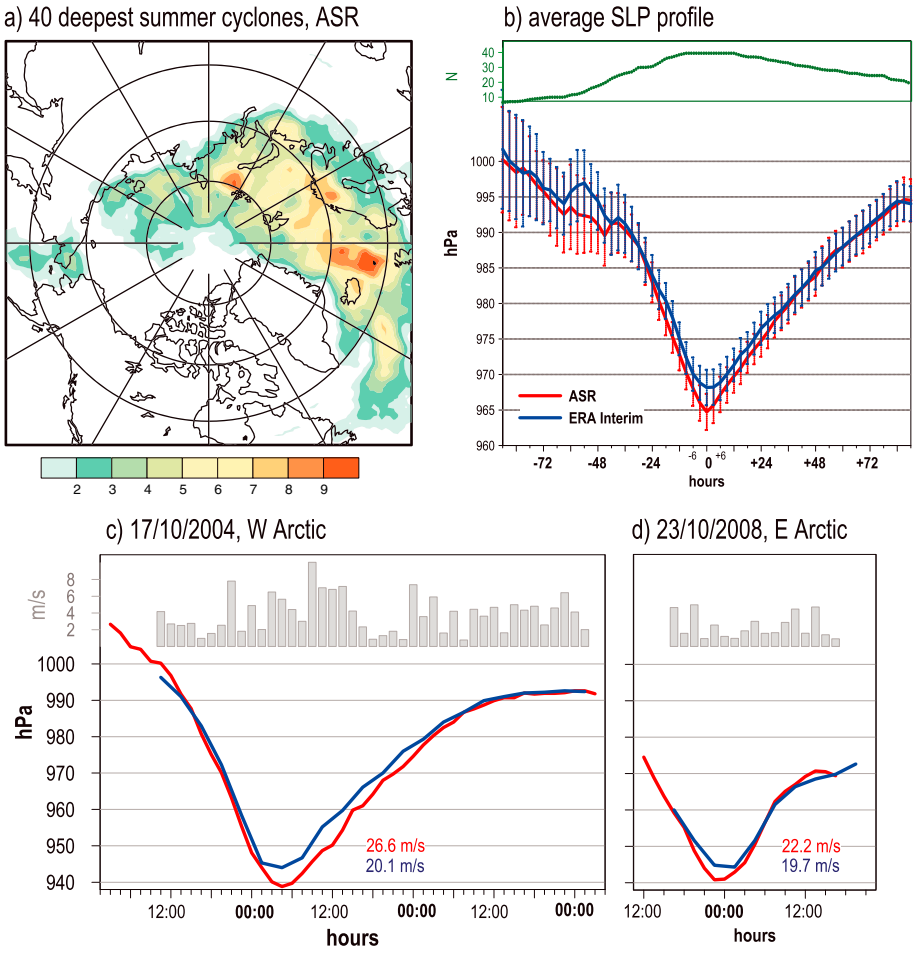

Figure 5. (a) Climatology of the number of cyclones (tracks per year per 155,000 km^2) for the 40 deepest summer cyclones during the period 2000–2010 from ASR reanalysis. (b) Evolution of the cyclone central pressure averaged over the 40 deepest cyclones. Vertical bars stand for the 95% confidence interval, and the green dotted line denotes the numbers of paired cyclone life cycle steps. (c and d) Evolution of the cyclone central pressure for the two case studies (17/10/2004 (Figure 5c) and 23/10/2008 (Figure 5d)). Grey bars show the difference in the maximum wind speed over the cyclone area between ASR and ERA-Interim.

in the Eastern Arctic (approximately between 120°E and 150°E), described by *Serreze and Barrett* [2008] and *Simmonds et al.* [2008]. In ERA-Interim this pattern is characterized by 30–40% smaller number of cyclones (8–11 cyclones per season) than in ASR (up to 18 cyclones) in summer. In winter this maximum is also less pronounced in ERA-Interim (8 cyclones per season) compared to ASR (up to 11 cyclones per season, Figures 3c and 3d). Over the Arctic Ocean winter differences between ASR and ERA-Interim are minor (2–4 cyclones per year, 25%), and they increase in summer up to 5–8 cyclones per year (30%).

Analysis of cyclone life cycle characteristics shows that on average ERA-Interim cyclones are slightly deeper compared to ASR. The lower central pressure in ERA-Interim results primarily from the larger population of shallow and moderately deep cyclones over the continents captured by ASR compared to ERA-Interim (Figure 4). Thus, over the high-latitude continents the fraction of intense events (< 980 hPa) in ASR is around 10% (both summer and winter) that is smaller compared to ERA-Interim (14% and 22% in winter and summer, respectively). However, if we consider the Arctic Ocean, probability distributions of cyclone central pressure in the two reanalyses become much closer (Figures 4a and 4c) especially in winter. These distributions are indistinguishable at the 90% level according to the *k-s* test. The fraction of intense cyclones (<980 hPa) over the Arctic Ocean in winter exceeds 20% in both ASR and ERA-Interim.

It is interesting whether the characteristics of very deep cyclones influencing dynamics of sea ice in summer [*Simmonds and Rudeva*, 2012; *Zhang et al.*, 2013] are different in ASR compared to ERA-Interim. We analyzed

separately the 40 most intense events over the Arctic Ocean selected from the ASR and corresponding tracks from ERA-Interim tracking outputs for the 2000–2010 decade. Most of these cyclones (36) entered the Arctic Ocean from the North Atlantic, four originated in the North Pacific (Figure 5a). Most intense cyclones primarily propagated over the GIN Sea and the Eastern Arctic. Central pressure in these cyclones is lower in ASR than in ERA-Interim with the average difference at the moment of maximum cyclone development being 4 hPa (Figure 5b). This implies that the deepening rate of intense cyclones in ASR is stronger compared to ERA-Interim. Note here that we found climatological SLP over the Arctic in ASR is ~0.5 hPa lower compared to ERA-Interim. Of the 40 cyclones 25 can be classified as rapidly intensifying (deepening rate is higher than 6 hPa per 6 h) [*Sanders and Gyakum* 1980] in both ASR and ERA-Interim. However, the averaged maximum deepening rate is nearly 1 hPa per 6 h higher in ASR cyclones compared to their ERA-Interim counterparts (7.6 and 6.7 hPa per 6 h for ASR and ERA-Interim, respectively). Most of intense events in ASR have a longer lifetime compared to ERA-Interim implying that ASR allows for earlier identification of cyclones and potentially for tracking the events for a longer time during the decay stage.

Analysis of the two case studies (Figures 5c and 5d) demonstrates that ASR cyclones are deeper compared to ERA-Interim with the largest central pressure difference being 5.2 and 4.8 hPa. Intense cyclones in ASR are also characterized by stronger pressure gradients and stronger 10 m winds through the whole life cycle (Figures 5c and 5d). Estimates of the maximum wind speed over the cyclone area for the two case studies show that winds are 3.8 (Figure 5c) to 2.6 m/s (Figure 5d) stronger in ASR compared to ERA-Interim with the differences in maximum wind speed at the moment of maximum cyclone intensity being 6.5 and 2.5 m/s.

4. Summary and Conclusions

ASR provides a new vision of the cyclone activity in high latitudes, showing that the Arctic is more densely populated with cyclones, especially in summer, than suggested by the modern era global reanalyses. ASR reveals 35% more cyclones mostly due to capturing shallow and moderately deep cyclones over the high-latitude continental areas. Over the Arctic Ocean ASR reports slightly higher cyclone counts compared to the global reanalyses with the largest differences being identified in summer (up to 18%). This is in line also with results by *Shkolnik and Efimov* [2013] who compared cyclone activity in a high-resolution regional climate model with a global model. ASR captures summer maximum of cyclone activity described by *Serreze and Barrett* [2008] and *Simmonds et al*. [2008] with the cyclone count being up to 23 cyclones per year; in ERA-Interim this maximum is 30% weaker in summer. Importantly, this maximum over the same area (120–150°E) also exists in winter in ASR (up to 12 cyclones per year), while in ERA-Interim it is hardly detectable. The most intense cyclones captured by ASR are deeper compared to their counterparts in ERA-Interim, showing also stronger deepening and higher maximum wind speeds. In most cases, ASR provides earlier identification of an extreme cyclone and also captures the cyclone decay at the later stage. The major advances of ASR compared to the global reanalyses are somewhat higher resolution, nonhydrostatic model formulation, and a much larger amount of assimilated data. However, the current resolution of the ASR model (~30 km) is only somewhat higher compared to global reanalyses (will be considerably higher in the next ASR release), and the advances of nonhydrostatic formulation has a minor effect at this resolution. *Jung et al*. [2006] and *Tilinina et al*. [2013] demonstrated strong dependence of cyclone counts on the resolution for the spectral range of reanalyses of the first generation, rather than for the resolutions of modern era products. Thus, we conclude that the much richer data assimilation input is primarily what provides higher accuracy of the description of cyclone activity and cyclone life cycle in ASR.

Definitely, ASR provides a very good perspective on analyzing extreme cyclones, largely affecting regional sea ice cover [*Simmonds and Rudeva*, 2012; *Zhang et al*., 2013]. In this study we did not consider the ability of ASR to capture mesoscale high-latitude cyclones known as polar lows [*Emanuel and Rotunno*, 1989; *Rasmussen and Turner*, 2003]. Intuitively, high-resolution ASR with optimal physics should be more skillful in reproducing these mesoscale phenomena; however, to effectively identify and track them, the tracking algorithm has to be adjusted significantly to target short-lived and rapidly developing vortices as has been done in some pilot studies [*Zahn and von Storch*, 2008; *Xia et al*., 2012]. The algorithm development along with appearance of the next higher-resolution ASR releases (with 15–km version to be issued in early 2014) will open a new avenue in studies of polar lows. Another line in the future may include the analysis of interactions between high-latitude cyclones and sea ice in order to understand both cyclone effect on the sea ice conditions and the mechanisms of the Arctic Ocean

impact on cyclone activity, involving changes in diabatic heating over increasing (with declining ice cover) ice-free water area. With ASR time series getting longer compared to the present 11 years, these feedbacks can be considered in the context of interannual variability in characteristics of cyclone activity and sea ice cover.

Acknowledgments

This work was supported by the Russian Ministry of Education and Science under the contracts 14.B25.31.0026 and 11.G.34.31.0007. N.T. and S.K.G. also benefited from the support of a special excellence grant NS-396.2014.5, RFBR grant 12-05-91323, and the GREENICE project funded by the NordForsk Nordic Top Level Research Initiative, project 61841. D.H.B.'s participation in this research as well as production of the Arctic System Reanalysis was funded by NSF grants ARC-0733023 and 1144117. We appreciate comments and suggestions from the two anonymous reviewers. Contribution 1440 of Byrd Polar Research Center.

The Editor thanks two anonymous reviewers for their assistance in evaluating this paper.

References

Barnes, E. A. (2013), Revisiting the evidence linking Arctic amplification to extreme weather in midlatitudes, *Geophys. Res. Lett.*, *40*, 4734–4739, doi:10.1002/grl.50880.

Bromwich, D. H., K. M. Hines, and L.-S. Bai (2009), Development and testing of Polar WRF: 2. Arctic Ocean, *J. Geophys. Res.*, *114*, D08122, doi:10.1029/2008JD010300.

Bromwich, D., Y.-H. Kuo, M. Serreze, J. Walsh, L. S. Bai, M. Barlage, K. Hines, and A. Slater (2010), Arctic System Reanalysis: Call for community involvement, *Eos Trans. AGU*, *91*, 13–14.

Dee, D. P., et al. (2011), The ERA-Interim reanalysis: Configuration and performance of the data assimilation system, *Q. J. R. Meteorol. Soc.*, *137*, 553–597.

Deser, C., R. Tomas, M. Alexander, and D. Lawrence (2010), The seasonal atmospheric response to projected Arctic sea ice loss in the late twenty-first century, *J. Clim.*, *23*, 333–351.

Duchon, C. E. (1979), Lanczos filtering in one and two dimensions, *J. Appl. Meteorol.*, *18*, 1016–1022.

Emanuel, K. A., and R. Rotunno (1989), Polar lows as Arctic hurricanes, *Tellus A*, *41*(1), 1–17.

Francis, J. A., and S. J. Vavrus (2012), Evidence linking Arctic amplification to extreme weather in mid-latitudes, *Geophys. Res. Lett.*, *39*, L06901, doi:10.1029/2012GL051000.

Gulev, S. K., O. Zolina, and S. Grigoriev (2001), Extratropical cyclone variability in the Northern Hemisphere winter from the NCEP/NCAR reanalysis data, *Clim. Dyn.*, *17*, 795–809.

Hines, K. M., and D. H. Bromwich (2008), Development and testing of Polar WRF. Part I. Greenland Ice Sheet meteorology, *Mon. Weather Rev.*, *136*, 1971–1989, doi:10.1175/2007MWR2112.1.

Hines, K. M., D. H. Bromwich, L.-S. Bai, M. Barlage, and A. G. Slater (2011), Development and testing of Polar WRF. Part III. Arctic land, *J. Clim.*, *24*, 26–48, doi:10.1175/2010JCLI3460.1.

Hodges, K. I., R. W. Lee, and L. Bengtsson (2011), A comparison of extratropical cyclones in recent reanalyses ERA-Interim, NASA MERRA, NCEP CFSR, and JRA-25, *J. Clim.*, *24*, 4888–4906.

Jung, T., S. K. Gulev, I. Rudeva, and V. Soloviov (2006), Sensitivity of extratropical cyclone characteristics to horizontal resolution in the ECMWF model, *Q. J. R. Meteorol. Soc.*, *132*(619), 1839–1857.

Neu, U., et al. (2013), IMILAST—A community effort to intercompare extratropical cyclone detection and tracking algorithms: Assessing method-related uncertainties, *Bull. Am. Meteorol. Soc.*, *94*, 529–547, doi:10.1175/BAMS-D-11-00154.1.

Parkinson, C. L., and J. C. Comiso (2013), On the 2012 record low Arctic sea ice cover: Combined impact of preconditioning and an August storm, *Geophys. Res. Lett.*, *40*, 1356–1361, doi:10.1002/grl.50349.

Rasmussen, E. A., and J. Turner (Eds.) (2003), *Polar lows: Mesoscale Weather Systems in the Polar Regions*, Cambridge Univ. Press, Cambridge, U. K.

Rienecker, M. M., et al. (2011), MERRA: NASA's modern-era retrospective analysis for research and applications, *J. Clim.*, *24*, 3624–3648.

Rudeva, I., and S. K. Gulev (2007), Climatology of cyclone size characteristics and their changes during the cyclone life cycle, *Mon. Weather Rev.*, *135*, 2568–2587.

Saha, S., et al. (2010), The NCEP Climate Forecast System, *J. Clim.*, *19*, 3483–3517.

Sanders, F., and J. R. Gyakum (1980), Synoptic-dynamic climatology of the "bomb", *Mon. Weather Rev.*, *108*, 1589–1606.

Screen, J. A., and I. Simmonds (2013), Exploring links between Arctic amplification and mid-latitude weather, *Geophys. Res. Lett.*, *40*, 959–964, doi:10.1002/grl.50174.

Screen, J. A., I. Simmonds, and K. Keay (2011), Dramatic interannual changes of perennial Arctic sea ice linked to abnormal summer storm activity, *J. Geophys. Res.*, *116*, D15105, doi:10.1029/2011JD015847.

Screen, J. A., I. Simmonds, C. Deser, and R. Tomas (2013), The atmospheric response to three decades of observed Arctic sea ice loss, *J. Clim.*, *26*, 1230–1248.

Serreze, M. C. (1995), Climatological aspects of cyclone development and decay in the Arctic, *Atmos. Ocean*, *33*, 1–2, doi:10.1080/07055900.1995.9649522.

Serreze, M. C., and A. P. Barrett (2008), The summer cyclone maximum over the central Arctic Ocean, *J. Clim.*, *21*, 1048–1065.

Shkolnik, I. M., and S. V. Efimov (2013), Cyclonic activity in high latitudes as simulated by a regional atmospheric climate model: Added value and uncertainties, *Environ. Res. Lett.*, *8*, 045007, doi:10.1088/1748-9326/8/4/045007.

Simmonds, I., C. Burke, and K. Keay (2008), Arctic climate change as manifest in cyclone behavior, *J. Clim.*, *21*, 5777–5796, doi:10.1175/2008JCLI2366.1.

Simmonds, I., and I. Rudeva (2012), The great Arctic cyclone of August 2012, *Geophys. Res. Lett.*, *39*, L23709, doi:10.1029/2012GL054259.

Stroeve, J., M. M. Holland, W. Meier, T. Scambos, and M. Serreze (2007), Arctic sea ice decline: Faster than forecast, *Geophys. Res. Lett.*, *34*, L09501, doi:10.1029/2007GL029703.

Tilinina, N., S. K. Gulev, I. Rudeva, and P. Koltermann (2013), Comparing cyclone life cycle characteristics and their interannual variability in different reanalyses, *J. Clim.*, *26*, 6419–6438.

Wilson, A. B., D. H. Bromwich, and K. M. Hines (2012), Evaluation of Polar WRF forecasts on the Arctic System Reanalysis Domain: 2. Atmospheric hydrologic cycle, *J. Geophys. Res.*, *117*, D04107, doi:10.1029/2011JD016765.

Xia, L., M. Zahn, K. I. Hodges, and F. Feser (2012), A comparison of two identification and tracking methods for polar lows, *Tellus A*, *64*, 17196, doi:10.3402/tellusa.v64i0.17196.

Zahn, M., and H. von Storch (2008), A long-term climatology of North Atlantic polar lows, *Geophys. Res. Lett.*, *35*, L22702, doi:10.1029/2008GL035769.

Zhang, J., R. Lindsay, A. Schweiger, and M. Steele (2013), The impact of an intense summer cyclone on 2012 Arctic sea ice retreat, *Geophys. Res. Lett.*, *40*, 720–726, doi:10.1002/grl.50190.

Zhang, X., J. E. Walsh, J. Zhang, U. S. Bhatt, and M. Ikeda (2004), Climatology and interannual variability of Arctic cyclone activity: 1948–2002, *J. Clim.*, *17*, 2300–2317.

Zolina, O., and S. K. Gulev (2002), Improving the accuracy of mapping cyclone numbers and frequencies, *Mon. Weather Rev.*, *130*, 748–759.